12

Metamaterial Waveguides and Antennas

Alexey A. Basharin, Nikolay P. Balabukha,
Vladimir N. Semenenko and Nikolay L. Menshikh
Institute for Theoretical and Applied Electromagnetics RAS
Russia

1. Introduction

In 1967, Veselago (1967) predicted the realizability of materials with negative refractive index. Thirty years later, metamaterials were created by Smith et al. (2000), Lagarkov et al. (2003) and a new line in the development of the electromagnetics of continuous media started. Recently, a large number of studies related to the investigation of electrophysical properties of metamaterials and wave refraction in metamaterials as well as and development of devices on the basis of metamaterials appeared Pendry (2000), Lagarkov and Kissel (2004). Nefedov and Tretyakov (2003) analyze features of electromagnetic waves propagating in a waveguide consisting of two layers with positive and negative constitutive parameters, respectively. In review by Caloz and Itoh (2006), the problems of radiation from structures with metamaterials are analyzed. In particular, the authors of this study have demonstrated the realizability of a scanning antenna consisting of a metamaterial placed on a metal substrate and radiating in two different directions. If the refractive index of the metamaterial is negative, the antenna radiates in an angular sector ranging from –90 ° to 0°; if the refractive index is positive, the antenna radiates in an angular sector ranging from 0° to 90° . Grbic and Eleftheriades (2002) for the first time have shown the backward radiation of CPW- based NRI metamaterials. A. Alu et al.(2007), leaky modes of a tubular waveguide made of a metamaterial whose relative permittivity is close to zero are analyzed. Thus, an interest in the problems of radiation and propagation of structures with metamaterials is evident. The purposes of this study is to analyze propagation of electromagnetic waves in waveguides manufactured from metamaterials and demonstrate unusual radiation properties of antennas based on such waveguides.

2. Planar metamaterial waveguide. Eigenmodes of a planar metamaterial waveguide

For the analysis of the eigenmodes of metamaterial waveguides, we consider a planar magnetodielectric waveguide. The study of such a waveguide is of interest because, if the values of waveguide parameters are close to limiting, solutions for the waveguides with more complicated cross sections are very close to the solution obtained for a planar waveguide, Markuvitz (1951). Moreover, calculation of the dispersion characteristics of a rectangular magnetodielectric waveguide with an arbitrary cross section can be approximately reduced to calculation of the characteristics of a planar waveguide.

Let us consider a perfect (lossless) planar magnetodielectric waveguide (Fig. 1), Wu et al. (2003). A magnetodielectric (metamaterial) layer with a thickness of $2a_1$ is infinite along the y and z axes. The field is independent of coordinate y.

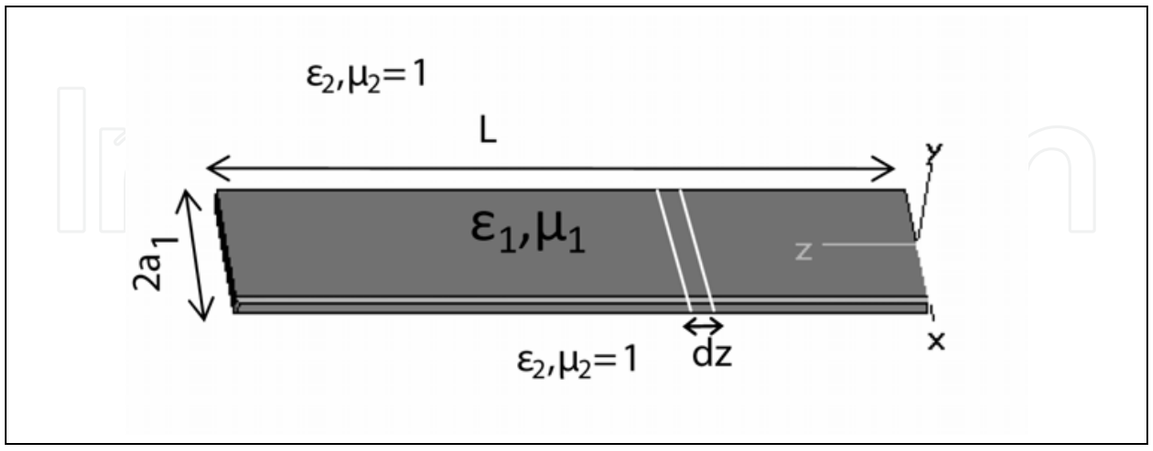

Fig. 1. A planar metamaterial waveguide.

The relative permittivity of this layer is ε_1 and the relative permeability is μ_1. The relative permittivity and relative permeability of the ambient space are ε_2 and μ_2, respectively. Let us represent the field in the waveguide in terms of the longitudinal components of the electric Hertz vector. For even TM modes, we write

$$\Pi_z^e = A_1 \sin(k_1 x)\exp(ihz) \text{ for } |x| < a_1 \tag{1}$$

$$\Pi_z^e = B\exp(-k_2|x|)\exp(ihz) \text{ for } |x| > a_1, \tag{2}$$

For odd TM modes, we have

$$\Pi_z^e = A_2 \cos(k_1 x)\exp(ihz) \text{ for } |x| < a_1 \tag{3}$$

$$\Pi_z^e = B\exp(-k_2|x|)\exp(ihz) \text{ for } |x| > a_1, \tag{4}$$

Where $k_0 = 2\pi/\lambda$ is the wave number in vacuum, λ is the wavelength, h is the longitudinal wave number,

$$k_1 = \sqrt{k_0^2 \varepsilon_1 \mu_1 - h^2}, \tag{5}$$

and

$$k_2 = \sqrt{h^2 - k_0^2 \varepsilon_2 \mu_2}. \tag{6}$$

Hereinafter, time factor exp*(-iωt)* is omitted.
The field components are expressed through the Hertz vectors as

$$E_x = \frac{\partial}{\partial x}\left(\frac{\partial \Pi_z^e}{\partial z}\right)$$
$$E_z = k_0^2 \varepsilon \mu \Pi_z^e + \frac{\partial}{\partial z}\left(\frac{\partial \Pi_z^e}{\partial z}\right). \quad (7)$$
$$H_y = ik_0 \varepsilon \frac{\partial \Pi_z^e}{\partial x}$$

Using the continuity boundary condition for tangential components *Ez* and *Hy* calculated from formulas (1), (2), and (7) at the material–free-space interface (at $x=a_1$), we obtain the characteristic equation for even TM modes

$$k_2 a_1 = k_1 a_1 \frac{\varepsilon_2}{\varepsilon_1} \mathrm{tg}(k_1 a_1) \quad (8)$$

It follows from formulas (3), (4), and (7) that, for odd TM modes,

$$k_2 a_1 = -k_1 a_1 \frac{\varepsilon_2}{\varepsilon_1} \frac{1}{\mathrm{tg}(k_1 a_1)} \quad (9)$$

Using also the continuity condition for longitudinal wave number *h*, we find from (5) and (6) that

$$(k_1 a_1)^2 + (k_2 a_1)^2 = (k_0 a_1)^2 (\varepsilon_1 \mu_1 - \varepsilon_2 \mu_2) > 0 \quad (10)$$

Equations (8), (10) and (9), (10) can be used to determine transverse wave numbers k_1 and k_2 for even and odd TM modes, respectively. Solutions to systems (8), (10) and (9), (10) will be obtained using a graphical procedure. Figure 2 presents the values of k_2a_1 as a function of k_1a_1. Solid curves *1,2,3*, etc., correspond to Eqs. (8) and dashed curves *A,B,C*, etc., correspond to Eq. (10), for even TM modes.

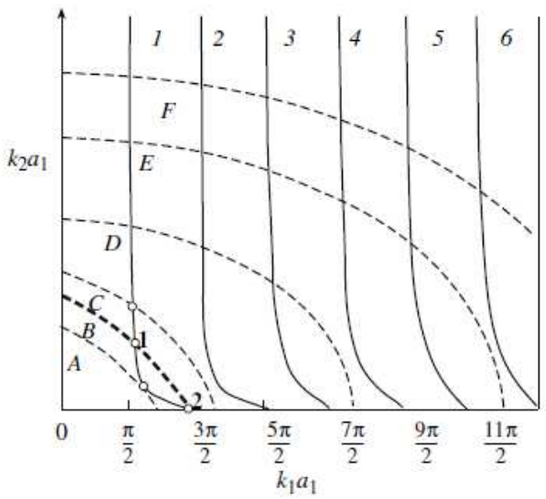

Fig. 2. Solution of the characteristic equations (8),(10).

Some curves (for example, curves *1* and *A* and curves *1* and *C*) may intersect at one point. These curves will be referred to as solutions of types I and II. Some curves (for example, curves *1* and *3*) may intersect at two points. These curves will be referred to as solutions of type III.

Let us consider the behavior of the power flux in such a waveguide for solutions I, II, and III. For the TM modes, the Poynting vector in the direction of the z axis is

$$S_z = \mathrm{Re}(E_x H_y^*) \tag{11}$$

For the layer of metamaterial,

$$S_{z1}(x) = A^2 \cos^2(k_1 x) h k_1^2 k_0 \varepsilon_1 \tag{12}$$

For the ambient space,

$$S_{z2}(x) = B^2 \exp(-2k_2 x) h k_2^2 k_0 \varepsilon_2 \tag{13}$$

The power flux is an integral over the waveguide cross section. The total power flux is

$$S_\Sigma = A^2 k_1^2 h k_0 \varepsilon_1 [\frac{a_1}{2} + \frac{\sin(2k_1 a_1)}{4k_1}] + B^2 k_2^2 h k_0 \varepsilon_2 \frac{\exp(-2k_2 a_1)}{2k_2}, \tag{14}$$

where the first term corresponds to the power flux in the metamaterial and the second term corresponds to the power flux in the ambient space.

Using the boundary condition, we can express coefficient A in terms of coefficient B. As a result, expression (14) transforms to

$$S_\Sigma = B^2 h k_0 \exp(-2k_2 a_1)[\frac{k_2^2 \varepsilon_1}{k_1^2 \sin^2(k_1 a)}(\frac{a_1}{2} + \frac{\sin(2k_1 a_1)}{4k_1}) + \frac{\varepsilon_2}{2k_2}] \tag{15}$$

For $\varepsilon_1 < 0$ and a chosen value of parameter h, the total flux can be either positive or negative. In the case of solution II, the total flux is negative, i.e., a backward wave propagates in the negative direction of the z axis, Shevchenko V.V (2005). Unlike dielectric waveguides, there are frequencies at which metamaterial waveguides can support two simultaneously propagating modes. Point **1** of solution III (see Fig. 2) corresponds to a negative power flux (a backward wave) and point **2** corresponds to a positive power flux (a forward wave). Solution I corresponds to zero flux, i.e., formation of a standing wave.

If the total flux takes a negative value, the negative value of wave number h should be chosen, Shevchenko V.V (2005).

Thus, depending on frequency, a planar metamaterial waveguide can support forward, backward, or standing waves. If constitutive parameters are negative, flux (12) and (13) are opposite to each other along the z axis. Accordingly, it can be expected that an antenna based on a planar metamaterial waveguide will radiate in the forward direction when flux $S_{z2}(x)$ (13) takes positive values; otherwise, it will radiate in the backward direction when $S_{z2}(x)$ takes negative values. Here, the total power flux is assumed to be positive.

3. Radiation of antenna based on planar metamaterial waveguide

Antennas manufactured on the basis of planar waveguides belong to the class of traveling-wave antennas, Balanis (1997). In calculation of the radiation patterns of such antennas, we

can approximately assume that the field structure in the antenna is the same as the field structure in an infinitely long planar waveguide. A planar waveguide supports TM and TE propagating modes. These modes are reflected at the end of the antenna rod, Balanis (1997), Aizenberg (1977). Under given assumptions, the radiation pattern of an antenna based on a metamaterial waveguide (the dependence of the field intensity measured in dB on azimuth angle θ measured in degrees) is calculated from the following formula:

$$f(\theta)=\frac{2}{k_0 L}\left(\frac{\sin(k_0\frac{L}{2}(\frac{h}{k_0}-\cos\theta))}{\frac{h}{k_0}-\cos\theta}+p\exp(iLh)\frac{\sin(k_0\frac{L}{2}(\frac{h}{k_0}+\cos\theta))}{\frac{h}{k_0}+\cos\theta}\right)f_1(\theta)\,, \tag{16}$$

where L is the antenna length, $f_1(\theta)$ is the radiation pattern of a antenna element dz (Fig. 1), obtained by a Hyugens` principle, and p is the reflection coefficient for reflection from the antenna end. p is defined under Fresnel formula. The second term (16) considers radiation of the reflected wave from a end of a waveguide, traveling in a negative direction z. Usually, the sizes and an antenna configuration chooses in such a manner that intensity of the reflected wave is small, Volakis J. A. (2007). And in practice the formula 17 is used:

$$f(\theta)=\frac{2}{k_0 L}\left(\frac{\sin(k_0\frac{L}{2}(\frac{h}{k_0}-\cos\theta))}{\frac{h}{k_0}-\cos\theta}\right)f_1(\theta)\,. \tag{17}$$

Formulas 16 and 17 are lawful for a case of small difference of a field in a vicinity of the end of a waveguide from a field in a waveguide. These formulas yield exact enough results only at small values of $a_1\sqrt{\varepsilon_1\mu_1}$, Angulo (1957).

Figures 3–7 show calculated *H*-plane radiation patterns of the antenna (based on planar metamaterial waveguide) for the TM modes. The patterns are normalized by their maximum values. The patterns obtained for the TE modes are qualitatively identical to the patterns corresponding to the TM modes and are not presented. The waveguide dimensions are a_1 = 50 mm and L = 400 mm, the relative permittivity of the metamaterial is ε_1 = –2, and the relative permeability of the metamaterial is μ_1 = –1. Calculation was performed at the following frequencies: 2.5, 2.8, 3.0, and 3.5 GHz.

Let us consider evolution of the radiation pattern of this antenna with frequency. A frequency of 2.5 GHz corresponds to solution I and zero total power flux. A standing wave is formed in the waveguide. This wave results from the interference of the forward and backward waves with wave numbers h having equal absolute values and opposite signs. The radiation pattern corresponding to the forward wave ($h > 0$) is shown in Fig. 3a.

The radiation pattern corresponding to the backward wave ($h < 0$) is the radiation pattern of the forward wave rotated through 180° (Fig. 3b). The radiation pattern corresponding to the interference of the forward and backward waves is shown in Fig. 4.

As frequency increases, solution I splits into two solutions. The upper part (point **1**) of solution III corresponds to a backward wave. In this case, the negative value of parameter h should be chosen. The total power flux (15) is negative. Figure 5a presents the radiation pattern at a frequency of 2.8 GHz. The back lobe of this pattern exceeds the main lobe; the

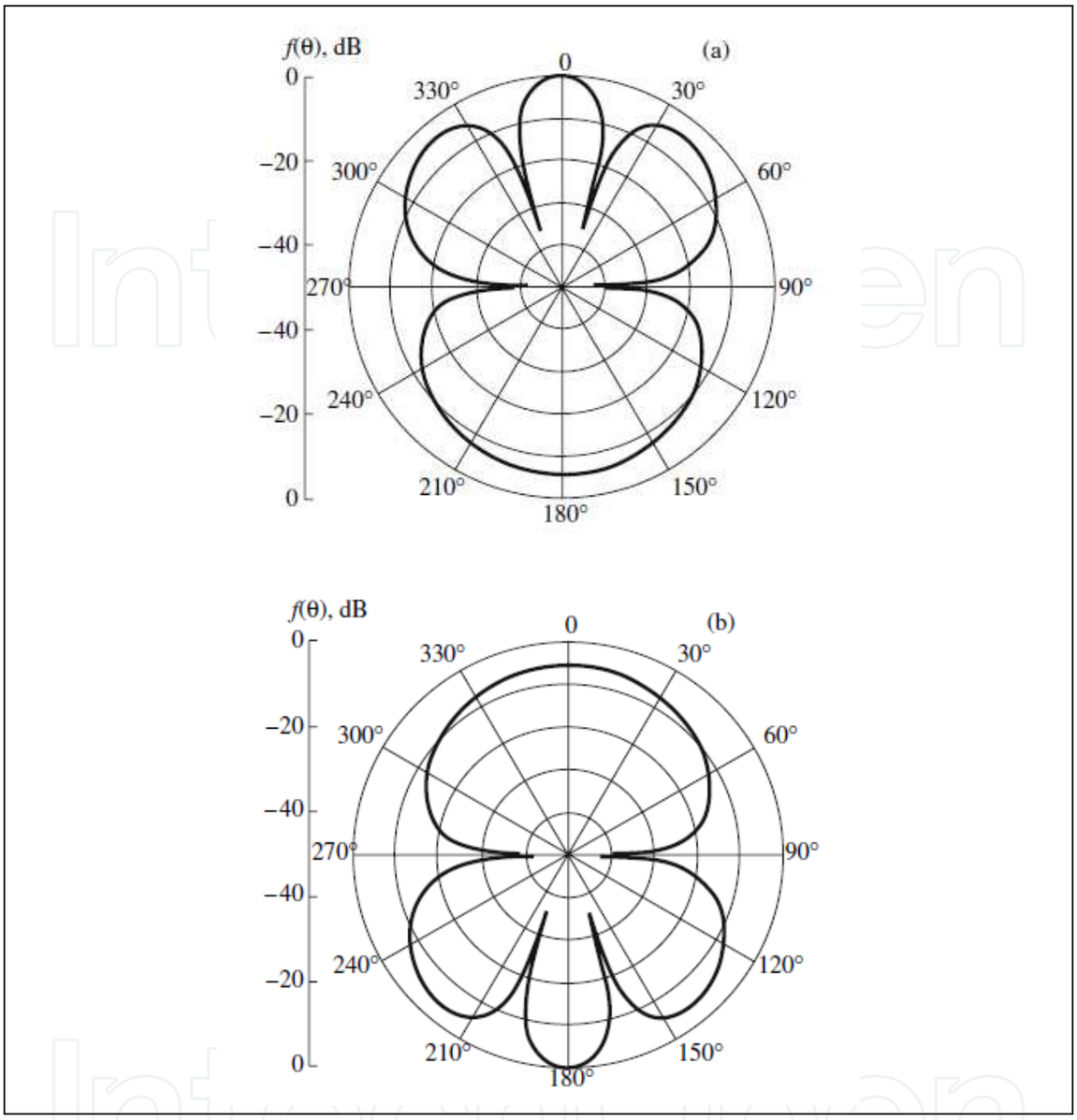

Fig. 3. Radiation patterns $f(\theta)$ on an antenna based on a planar metamaterial waveguide at a frequency of 2.5 GHz for solution I in the cases of (a) forward and (b) backward waves.

antenna radiation direction is 180°. The lower part (point **2**) of solution III corresponds to a forward wave. The positive value of longitudinal wave number h is chosen. The field is localized out of a waveguide and the total power flux (15) is positive. The maximum of the radiation pattern is located at 0° (Fig. 5b).

A frequency of 3.0 GHz corresponds also to solution III. In the case of the upper part (point **1**) of solution III, the antenna predominantly radiates in the backward direction (at 180°, see Fig. 6a). In the case of selection of the lower part (point **2**) of solution III, the antenna radiates in the main direction (at 0°, see Fig. 6b).

If frequency further increases, two-mode solution III transforms into single-mode solution II. In the case of solution II, the metamaterial waveguide supports a backward propagating

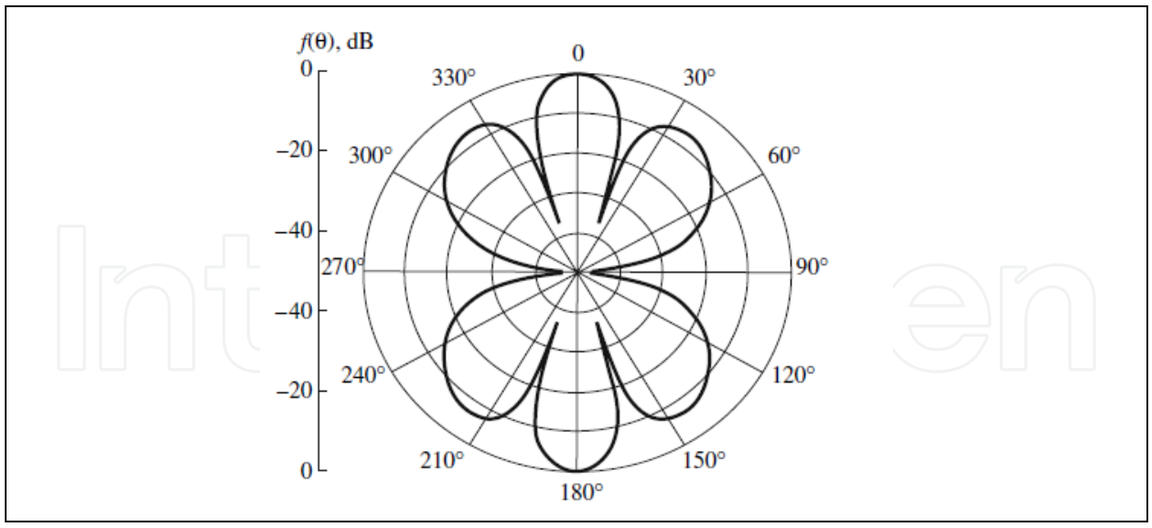

Fig. 4. Radiation pattern $f(\theta)$ on an antenna based on a planar metamaterial waveguide at a frequency of 2.5 GHz for solution I and interference of the forward and backward waves.

wave. The negative value of longitudinal wave number h should be chosen. The radiation pattern at a frequency of 3.5 GHz is shown in Fig. 7. The maximum of this radiation pattern is located at 180°.

It can be proved that this backward radiation effect in a direction of 180° is possible only for the antennas manufactured on the basis of metamaterial waveguides with negative values of the relative permittivity and relative permeability.

The condition of radiation in the backward direction (180°) is the inequality

$$f(\theta = 0) - f(\theta = 180) < 0\,, \tag{17}$$

which can readily be solved analytically by Basharin at al. (2010). The corresponding solution is

$$\varepsilon_1 < -\varepsilon_2 \frac{k_1^2}{k_2^2}\,. \tag{18}$$

It follows from expression (18) that backward radiation is possible only for negative values of permittivity ε_1 and under the condition ε_1, $\mu_1 < 0$. Analysis shows that condition (18) is not satisfied for solution I and point 2 of solutions III. In these cases, the antenna radiates in the main direction (see Figs. 3a, 5b, 6b).

As a practical application of this effect, we can propose a two-mode scanning antenna, which on one frequency, in the case of operation in the first mode (point **1** of solution III, see Fig. 2), can radiate in the backward direction (at 180°, see Figs. 5a, 6a) and, in the case of operation (at the same frequency) in the second mode (point **2**), can radiate in the main direction (at 0°, see Figs. 5b, 6b). Switching from one mode to another can be performed, for example, by feeding the antenna from a system of electric dipoles placed parallel to the electric field lines at the feeding point of the antenna. Changing the amplitude– phase distribution in each dipole, it is possible to obtain the field distribution required for the first or the second mode.

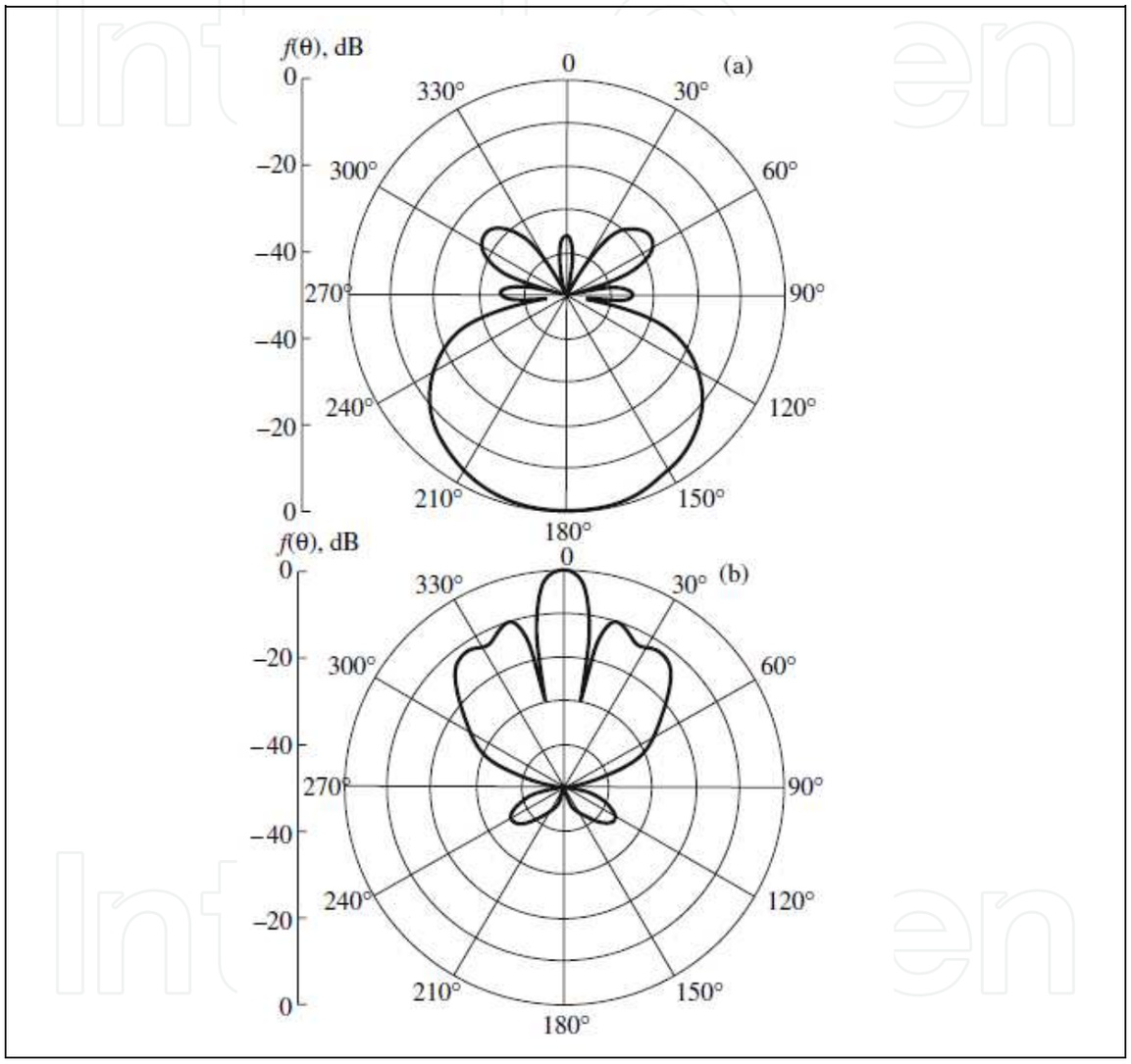

Fig. 5. Radiation patterns $f(\theta)$ on an antenna based on a planar metamaterial waveguide at a frequency of 2.8 GHz for solution III and points (a) **1** and (b) **2**.

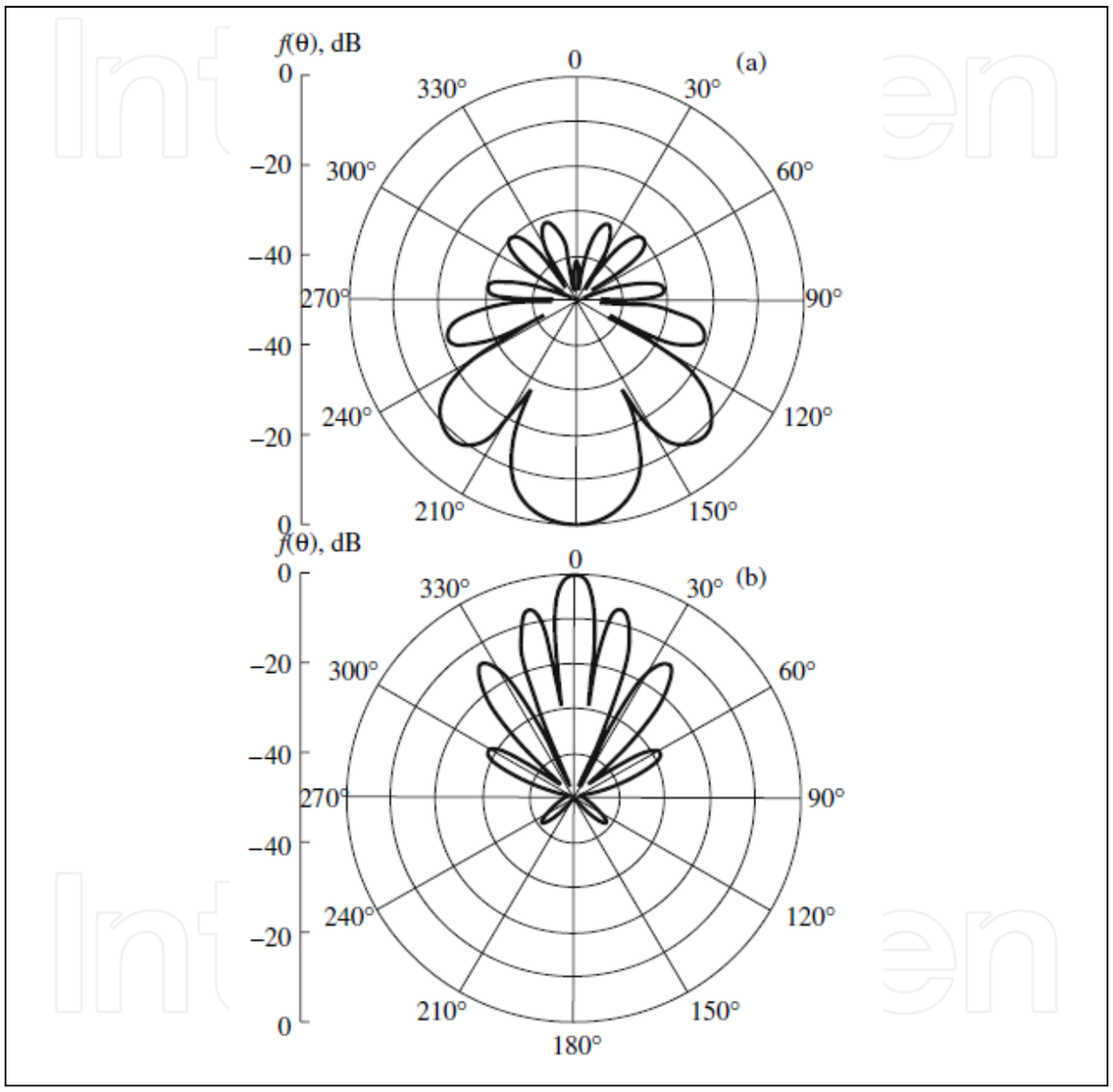

Fig. 6. Radiation patterns $f(\theta)$ on an antenna based on a planar metamaterial waveguide at a frequency of 3.0 GHz for solution III and points (a) **1** and (b) **2**.

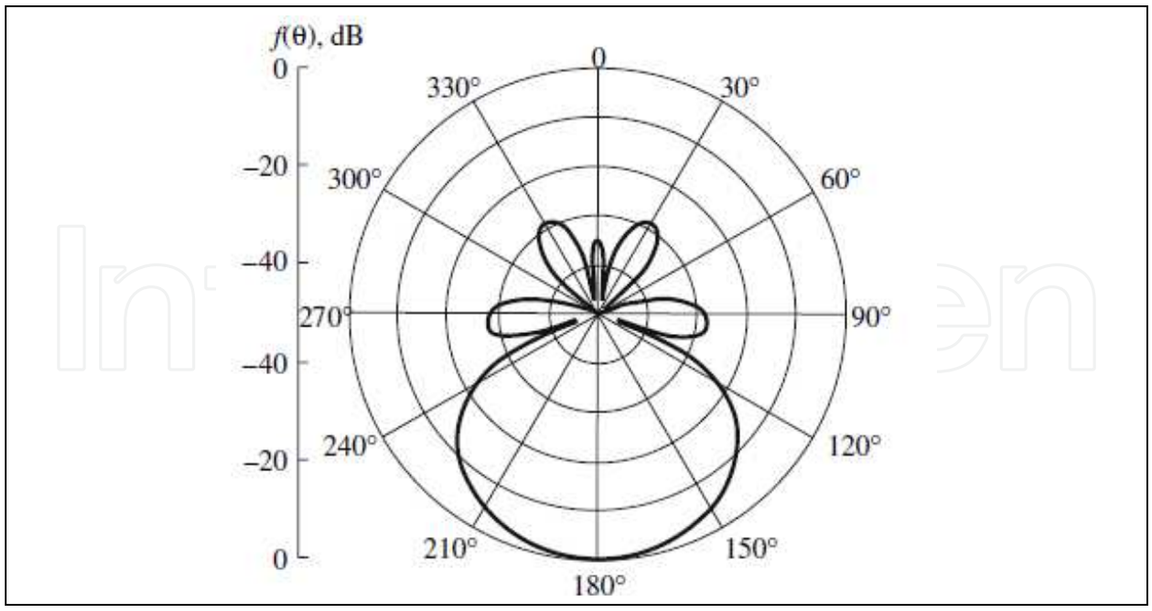

Fig. 7. Radiation pattern $f(\theta)$ on an antenna based on a planar metamaterial waveguide at a frequency of 3.5 GHz for solution II.

4. Characteristics of electromagnetic waves in a planar waveguide based on metamaterial with losses

Here we present results of calculation of dispersion characteristics for a planar waveguide made of metamaterials with losses and wave type classification in such waveguides. It demonstrates that forward and backward waves can exist in such structure, waves can permeate "without attenuation" (so the imaginary part of longitudinal wave number is near zero) in spite of presence losses in metamaterial, as well it shows presence of wave mode propagating with a constant phase velocity which does not depends on the frequency. This paper researches dispersion characteristics of the planar metamaterial waveguide with losses, analyses the waveguide characteristics and classifies wave modes.

Let's consider a planar waveguide, made of a metamaterial with losses (Fig. 1). The concerned metamaterial is not ideal and has losses, so its penetrability's are complex values and can be presented as: $\varepsilon_1=\varepsilon_1'+\varepsilon_1''$, $\mu_1=\mu_1'+\mu_1''$.

Having placed expressions (5) and (6) in equation (8) for k_1 and k_2 (continuity condition for the longitudinal wave number h) it should reduce to the following expression:

$$\cos\left[a\sqrt{k_0^2\varepsilon_1\mu_1-h^2}\right]\varepsilon_1\sqrt{h^2-k_0^2\varepsilon_2\mu_2}-\varepsilon_2\sqrt{k_0^2\varepsilon_1\mu_1-h^2}\sin\left[a\sqrt{k_0^2\varepsilon_1\mu_1-h^2}\right]=0 \qquad (19)$$

Equation (19) is solved with Muller method, Muller (1965), Katin and Titarenko (2006). In the capacity of initial estimate we choose values of h within the wide range from 0 to few k_0.

For the metamaterial waveguide with parameters ε'_1= *-2* and μ'_1= *-1* calculations have been done for various imaginary parts of penetrabilities. Results are presented as diagrams of h'/k_0 and h''/k_0 versus wave number of environment k_0a (Fig.8-13). Great numbers of waves,

which exist simultaneously at the same frequency in the waveguide, make us give special attention on their classification

Viewing the diagrams of imaginary and real parts of longitudinal wave number we see right lines $h'=k_0$ and $h''=k_0$ allowing to divide all waves into fast ($h'<k_0$) and slow ($h'>k_0$) waves, strongly attenuation waves ($h''>k_0$) and weak attenuation ones ($h''<k_0$), Marcuvitz (1951), Vainshtein (1988), Shevchenko (1969).

Let's consider the case when the metamaterial has not got any losses, Shadrivov et al. (2003), Basharin et al. (2010). At low frequencies all waves are backward (dotted lines on the diagrams), it means that the phase velocity direction is opposite to the Poynting vector. At some frequency (points A and B in Fig.8) the wave is split into two modes: forward (continuous line on the diagrams) and backward. Fields of these waves presented on Fig. 14 and Fig. 15. Away from waveguide the fields decay on exponential law. The both modes start to propagate without any losses. The forward wave exists only within the narrow frequency range. Further increasing of frequency forces the forward wave turn into the "anti-surface wave" (improper wave) (Away from waveguide the field grows exponentially), Vainshtein (1988), Marcuvitz (1951), which exists only mathematically (dash-dotted lines).

Z component of Poynting vector is negative inside the waveguide, but it is positive outside. There is a zero density of power flow at the splitting points (points A, B in Fig.8) i.e. a

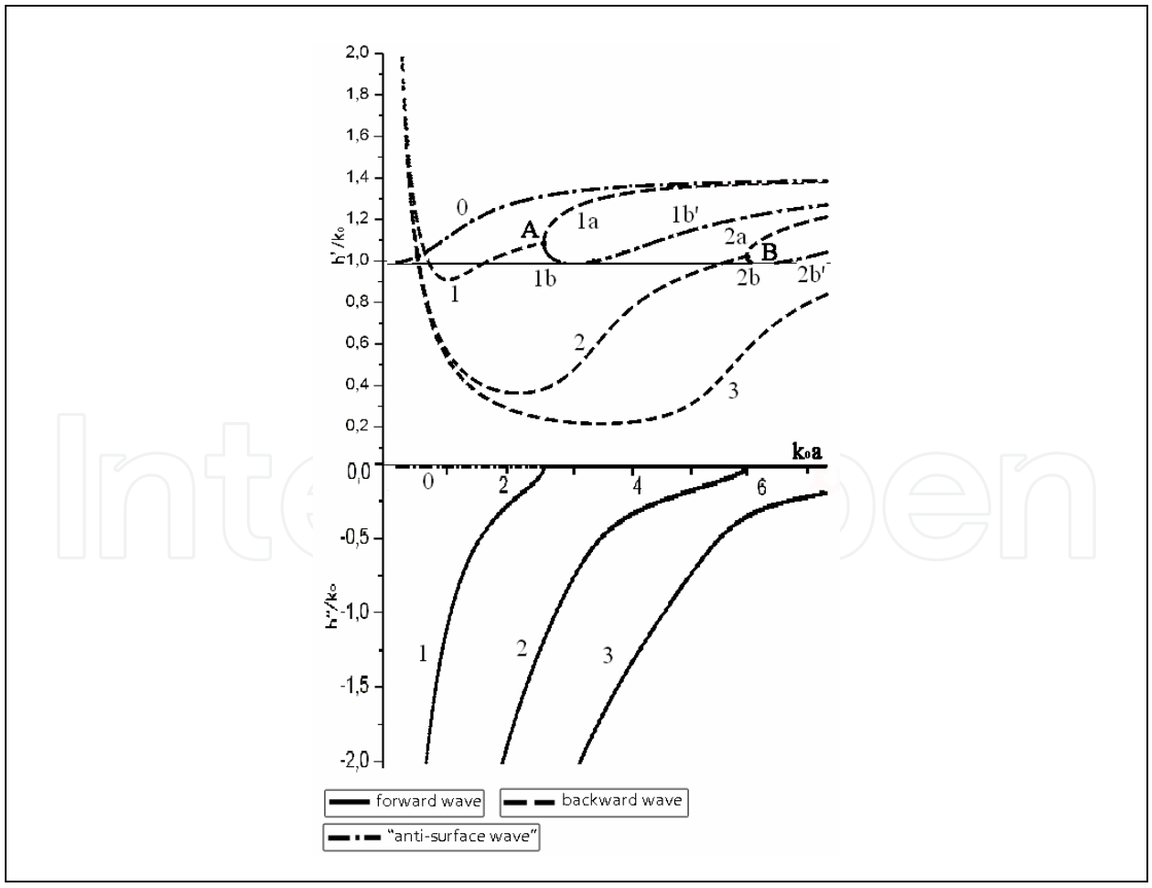

Fig. 8. Dispersion characteristic of metamaterial waveguide with ε_1=-2, μ_1=-1

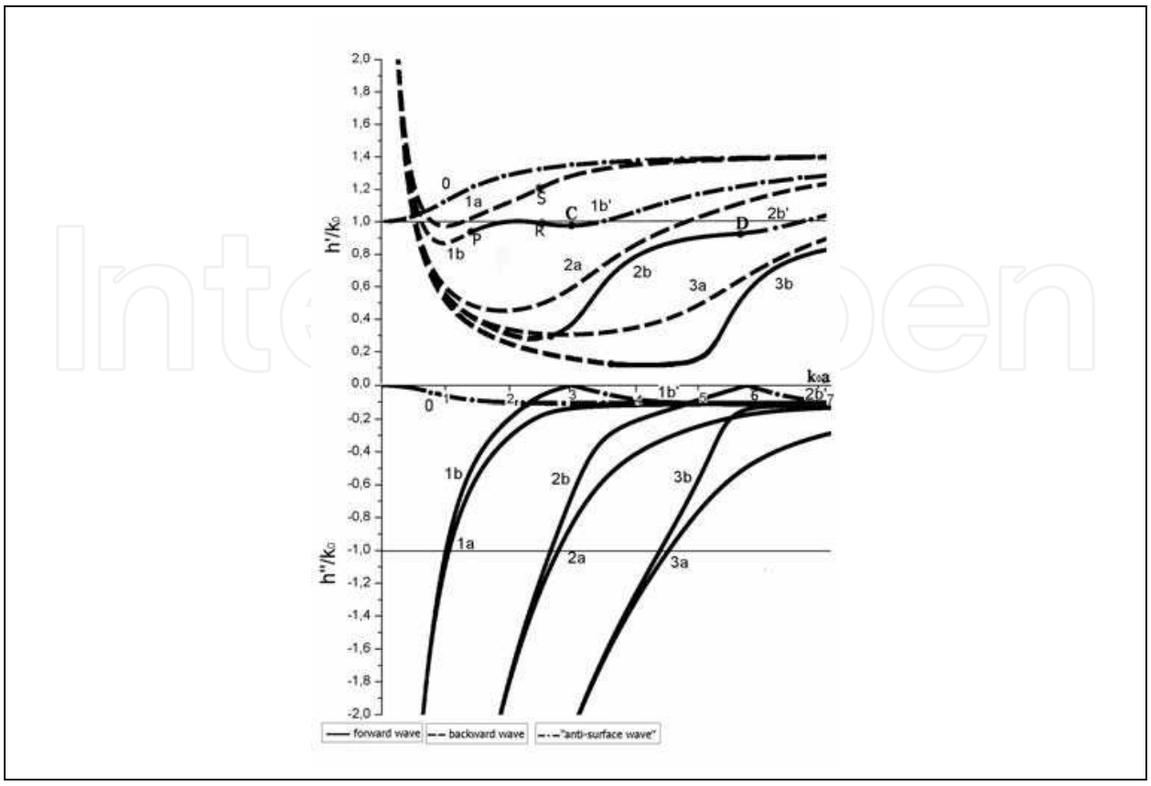

Fig. 9. Dispersion characteristic of metamaterial waveguide with ε_1=-2+i0.1, μ_1=-1+i0.1

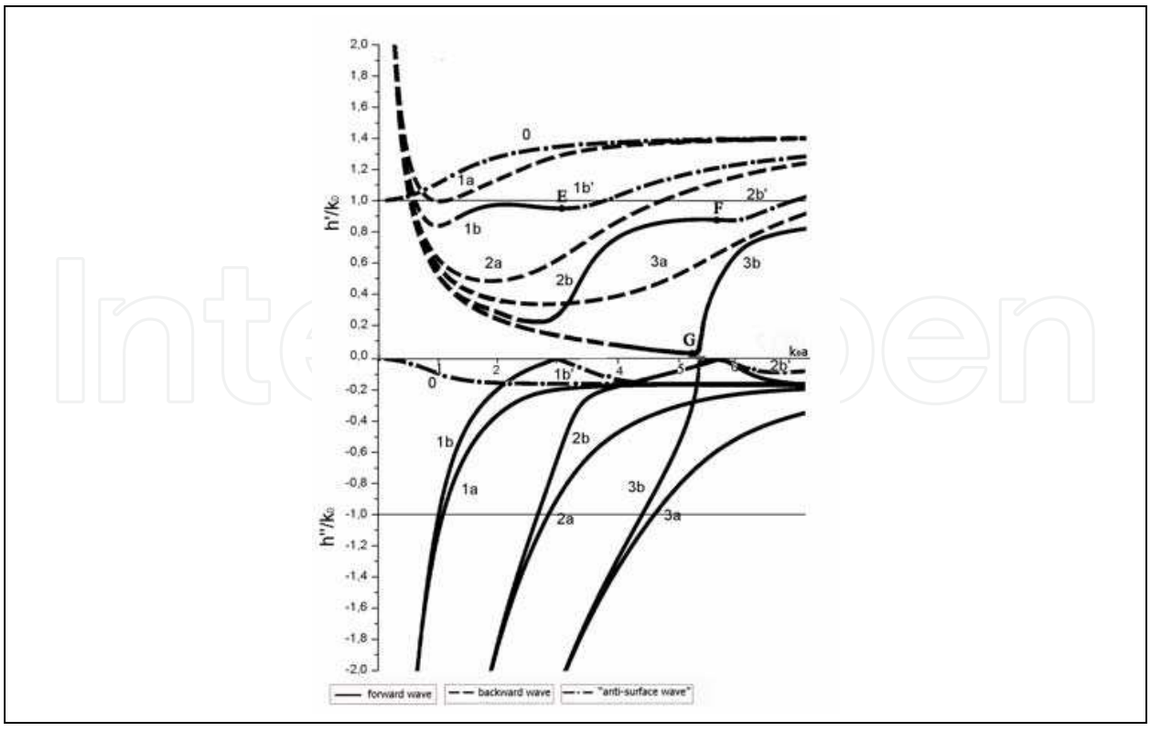

Fig. 10. Dispersion characteristic of metamaterial waveguide with ε_1=-2+i0.15, μ_1=-1+i0.15

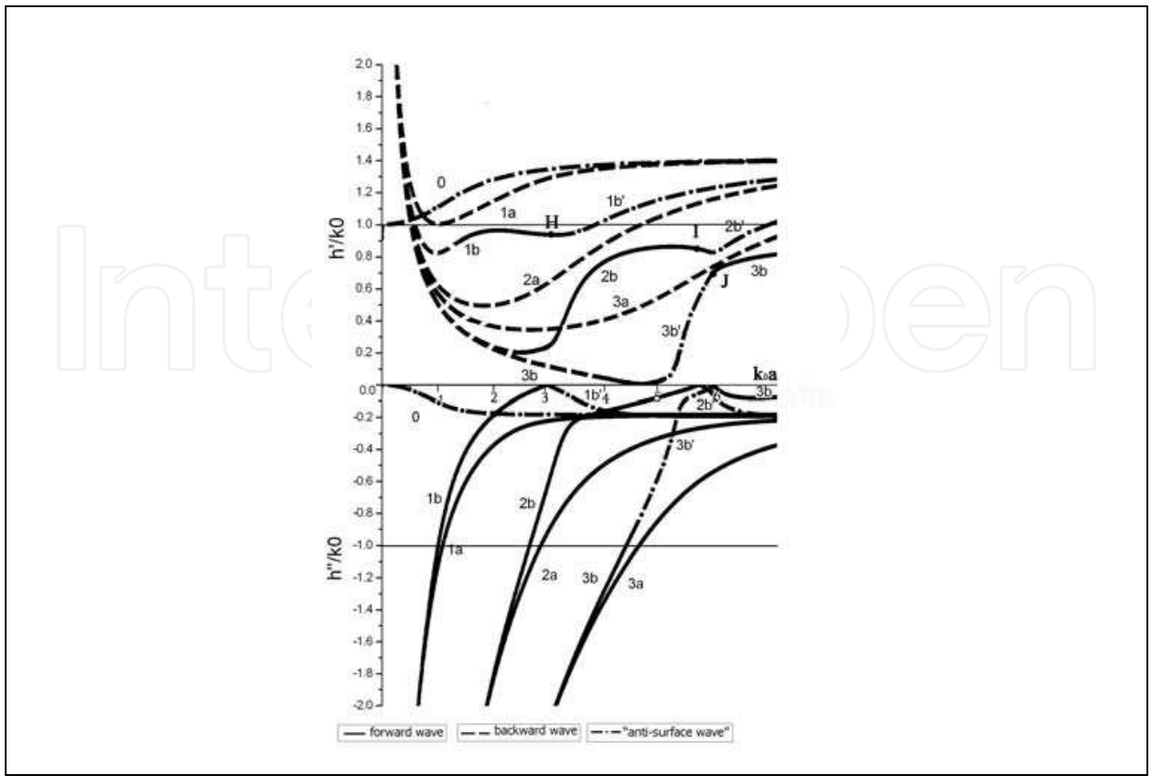

Fig. 11. Dispersion characteristic of metamaterial waveguide with ε_1=-2+i0.17, μ_1=-1+i0.17

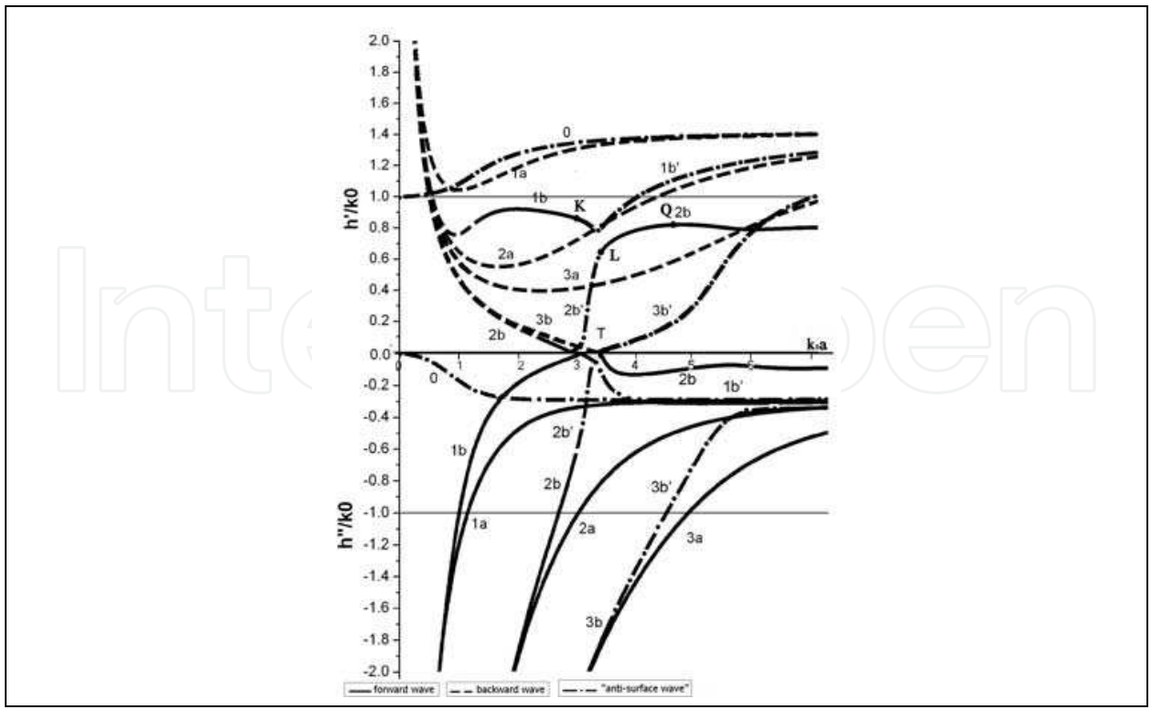

Fig. 12. Dispersion characteristic of metamaterial waveguide with ε_1=-2+i0.27, μ_1=-1+i0.27

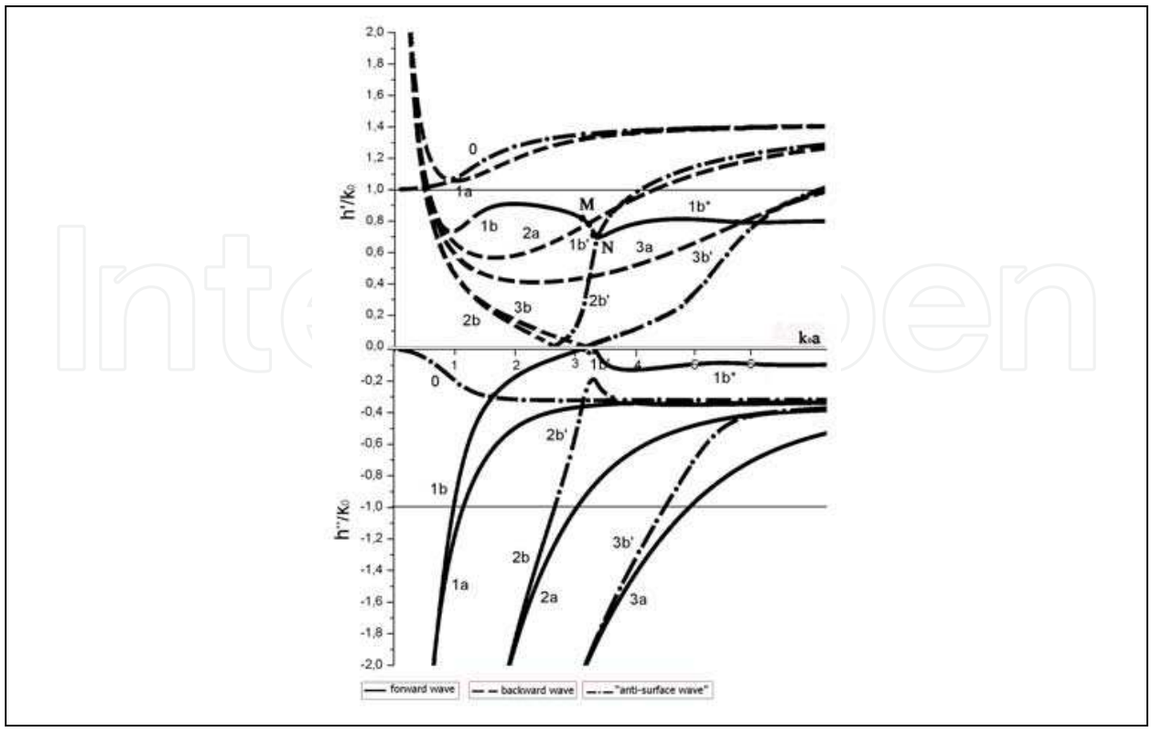

Fig. 13. Dispersion characteristic of metamaterial waveguide with ε_1=-2+i0.3, μ_1=-1+i0.3

standing wave arises as result of interference of the forward and backward wave, Basharin et al., (2010), Shatrov et al. (1974); Shevchenko at al. (2000).

When we include a loss in metamaterial, then splitting occurs at low frequencies. Both modes are supported in whole range (Fig. 9). One mode is backward and the second at a certain frequency is transformed into a forward (point P).

The range of frequencies in which there is forward wave increases as compared with the case without losses. The fields of these waves are the leaking (Fig. 16 a - forward, b - backward). These waves, as in the absence of losses, transformed in "anti-surface" ones with growing frequency. However, for sufficiently large losses wave decays before reaching the transition point in the forward wave. In this case (Fig. 12, point T) backward wave soon becomes "anti-surface".

Some results require further discussion. For sufficiently large losses (0.17 and over) for some modes there is a certain frequency range in which the forward wave is transformed into anti-surface wave. So a transition mode 3b in 3b' in Fig. 11 and fashion in 2b 2b' in Fig. 12.

Near at the change point where the surface wave turns into the "anti-surface" one and converse (excluding the point where $h'=0$) the wave field essentially concentrates outside the waveguide. Even considering the metamaterial inserts some losses, the wave can propagate without no degradation at these points, so the imaginary part of longitudinal wave number h'' is near zero (points C, D, E, F, H, G, I, J, K, L, M, N).

When the imaginary parts of penetrabilities are sufficiently great the wave modes are combined. At first two forward waves are combined with the "anti-surface wave" and when losses are being increased it disappears. It is obviously (Fig.11) the 2-nd and 3-rd modes are being combined and when the losses are great the 1-st and 2-nd modes are being combined (Figs.12, 13). These waves through exist lose in metamatirael ($\varepsilon''\neq0$, $\mu''\neq0$) exist points (for

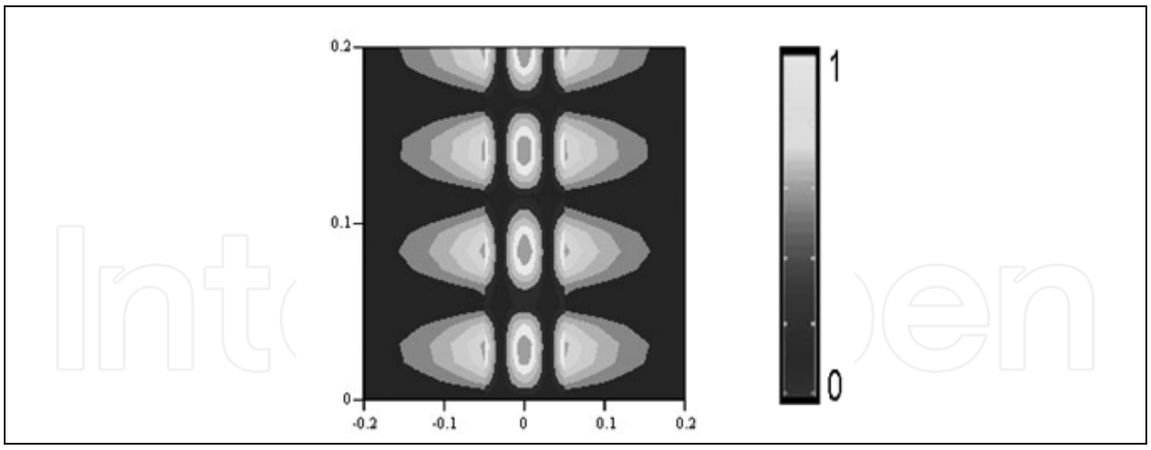

Fig. 14. Normalize magnetic field near point A (Fig. 8), forward wave.

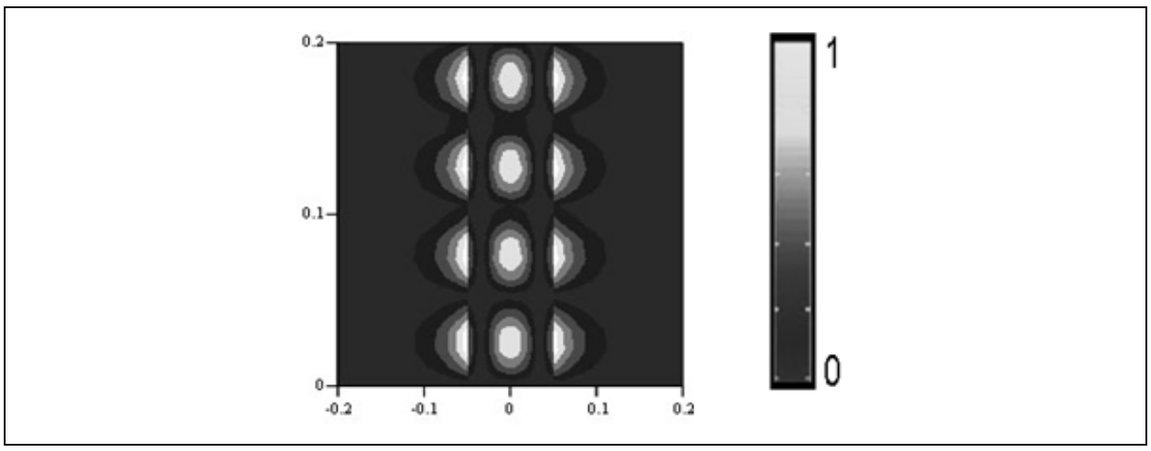

Fig. 15. Normalize magnetic field near point A (Fig. 8), backward wave

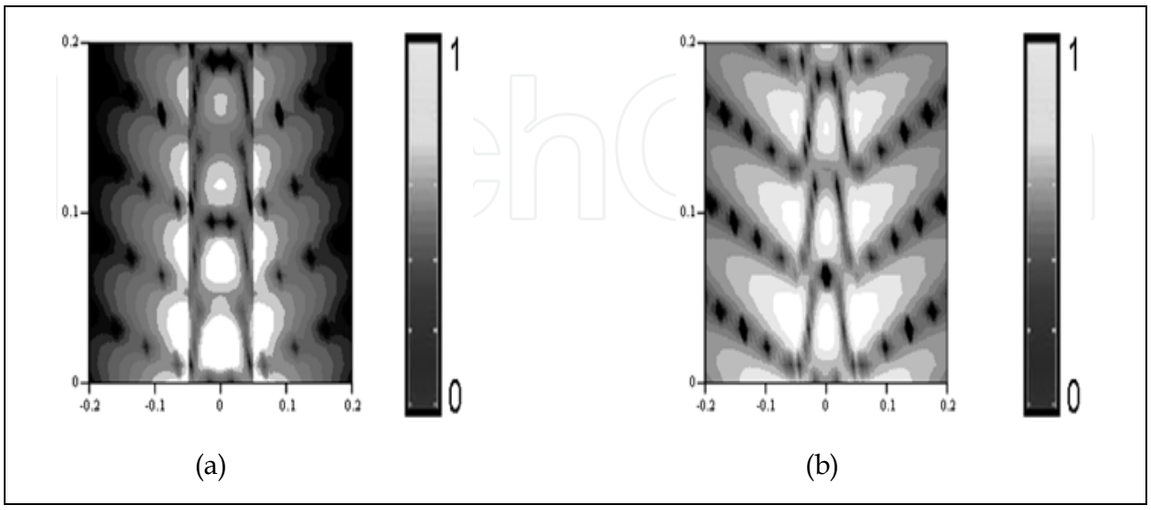

Fig. 16. Normalize magnetic field: a) backward wave, point S (Fig. 9); b) forward wave, point R (Fig. 9).

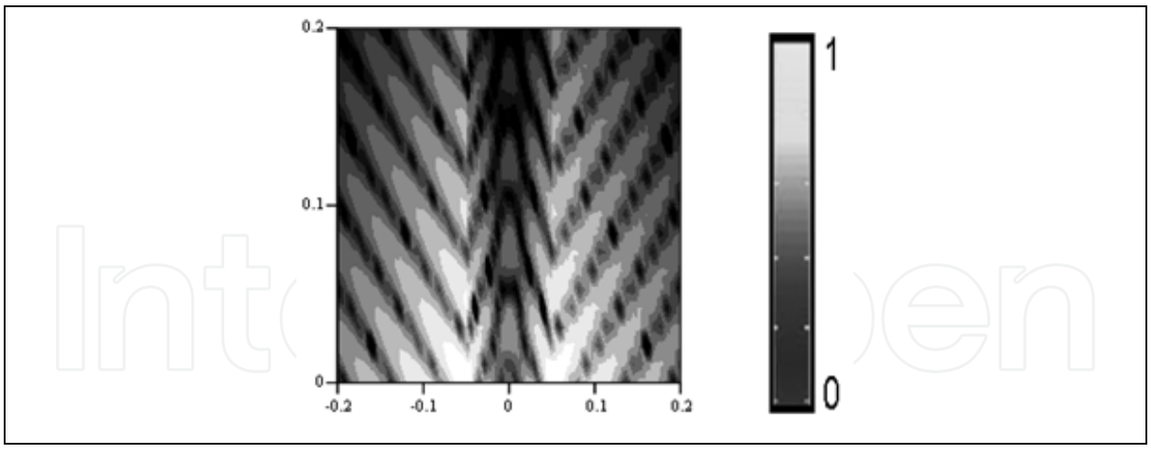

Fig. 17. Normalize magnetic field near point Q (Fig. 12).

example, point Q on Fig. 12) where imagine part of h is near zero. At this point the field is concentrated outside the waveguide (Fig. 17) and close to the free wave field.

While frequency increasing the phase velocity usually increases starting from the moment when the imaginary part h is getting sufficiently small to that waves can propagate. As for combined modes such relationship is not observed, the phase velocity remains almost constant while frequency increasing. Notably the velocity becomes constant with less loss, i.e. before waves combine near the modes 3b in Fig. 11 and 2b in Fig.12. Generally the fields and power flows for such waves are concentrated at the waveguide boundary. Outside the waveguide the field decays exponentially except abovementioned cases (points C, D, E, F, H, G, I, J, K, L, M, N).

Also, the mathematic models of wave types for planar waveguide made of the metamaterials with losses was researched. It was shown that forward and backward waves can propagate in such structure. It was pointed out that waves can propagate with $h''=0$ at defined frequencies despite metamaterial inserts losses. Combining of wave types is observed while losses inserted, and the combined modes propagate at a constant phase velocity which does not depend on frequency. These waves are forward, but in contrast to other forward waves they do not turn into "anti-surface waves", but they exist through all the frequency range starting from some frequency. These's fields of practice isn't percolate in waveguide and concentrate on waveguide's bound.

To be noted that the real metamaterials have strong frequency dispersion, so the material with constant permeability through all the concerned frequency range can not be made. But a metamaterial with desired permeability can be made for limited frequency ranges. In such metamaterial all above mentioned properties will be observed.

5. Experimental verification of the backward wave radiation from a metamaterial waveguide structure

This work is aimed at the experimental verification of the effect of backward radiation of electromagnetic waves by the example of an antenna in the form of a rectangular tube based on a metamaterial with the thickness d and negative real parts of permittivity and permeability. The essence of the effect is the preferential backward radiation of the antenna structure. The numerical simulations (with the use of the method of moments) and the

measurements of the far field radiation patterns in the anechoic chamber show that such radiation is possible only at negative real parts of the permittivity and permeability of the metamaterial. However, at positive values, this antenna behaves like a usual dielectric antenna and radiates in the main direction. The geometry of the metamaterial tube waveguide antenna made is shown in Fig. 18.

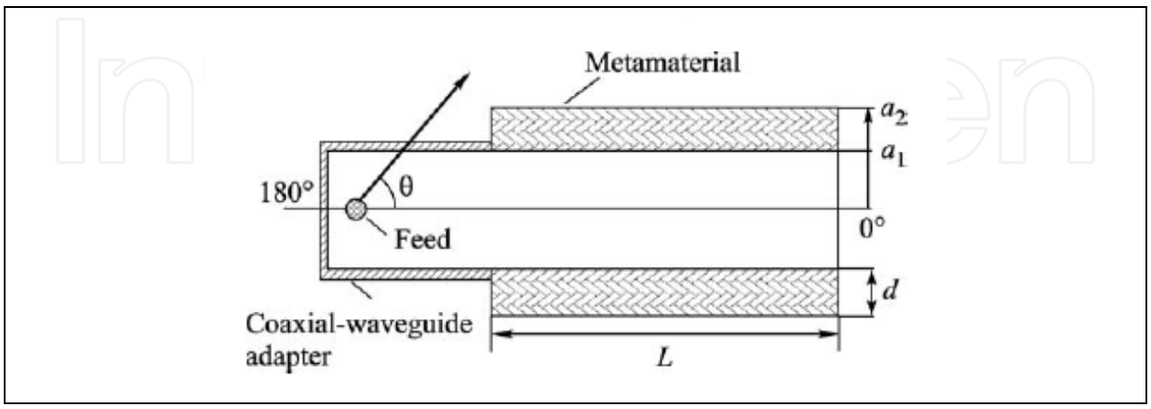

Fig. 18. Scheme of the metamaterial tube waveguide antenna.

The antenna was excited through a standard coaxial connection with a 50x25 mm waveguide for the 10 cm wavelength range. The tube length was L = 150 mm. The middle layer consisted of expanded polystyrene with a nearly unity relative permittivity. A photo of the antenna is shown in Fig. 19.

Fig. 19. Photo of the antenna under investigation.

The properties of an anisotropic metamaterial were described by Lagarkov A.N. et al. (2003). The distinctive features of the metamaterial used in this work are its spatially isotropic electric and magnetic resonance properties in the same frequency range. The metamaterial is an isotropic two dimensional array of Nichrome helixes placed on a thin 0.2 mm polyurethane substrate. To avoid the appearance of the metamaterial chirality, the right and left helixes were used in equal numbers. The helixes with an outer diameter of 5 mm consisted of three turns of a 0.4 mm Nichrome wire with a 1 mm pitch. A helixes with a nonzero pitch is simultaneously electric and magnetic dipoles, which may be effectively

excited by both electric and magnetic fields polarized along the helix axis. The electric and magnetic fields of a wave incident on the metamaterial layer excite the electric and magnetic dipole moments of the helix, whose axes are parallel to the vectors **E** and **H**, respectively. At frequencies somewhat above the resonance frequency of the helixes, the phase shift between the field of the incident wave and the field induced by the currents in the metamaterial elements becomes negative; as a result, the real parts of permittivity and permeability become negative, Gulyaev et al. (2008).

In the experiments, a 5.2 mm thick sheet metamaterial was used (see Fig. 20, the coils were directed along the *x*, *y*, and *z* axes in equal numbers). The parameters of the sample were chosen so as to provide the resonance of permittivity and permeability at a frequency of about 3 GHz.

Fig. 20. Appearance of the planar metamaterial sample.

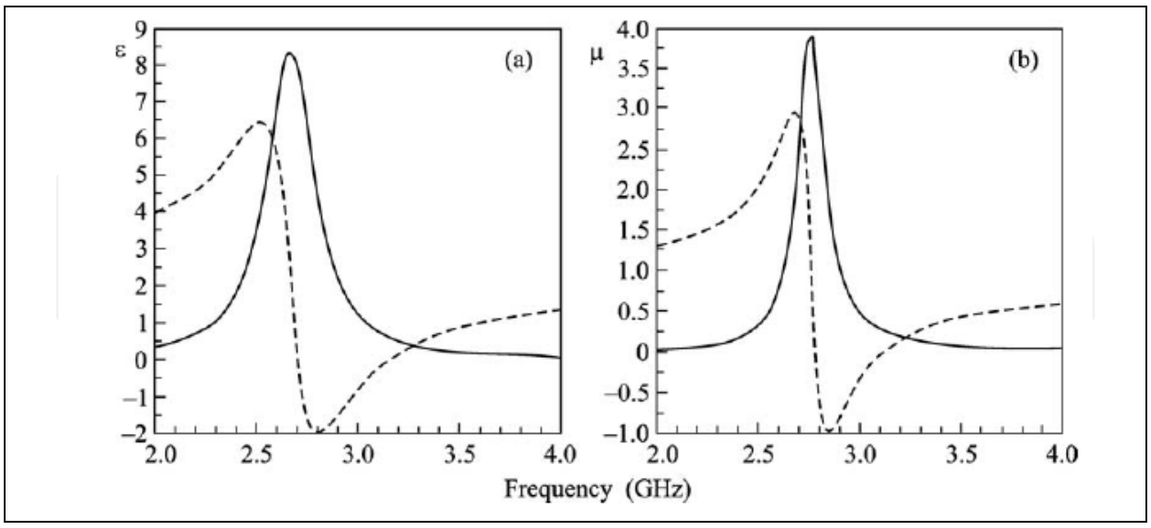

Fig. 21. Frequency dependence of the effective complex relative (a) permittivity and (b) permeability.

The experimental frequency dependence of the effective material parameters of the sample calculated from the measured values of the *S* parameters (complex reflection and

transmission coefficients) of the planar metamaterial sample according to the Fresnel formulas is shown in Fig. 21 (the dashed and solid lines represent the real and imaginary parts, respectively). According to the studies of sheet materials by Lagarkov et al. (1990, 1997, 2003), the results of measurements for two or more layers are not considerably different from those shown in Fig. 21 and are not presented here.

The permittivity and permeability of the metamaterial are negative near a frequency of 3 GHz. The measurements were carried out with the use of the previously developed and approved technique for measuring the permittivity and permeability of sheet materials in the near field of horn antennas based on the measurement of *S* parameters. The technique was implemented with the use of a Rhode & Schwarz ZVA 24 four port Vector Network Analyzer. According to the test measurements with reference samples, the experimental error of permittivity and permeability was no more than 5%.

Let us consider the fields propagating in the waveguide part of the antenna. The calculation of the characteristics of the rectangular metamaterial waveguide may be approximately reduced to the calculation of the characteristics of the planar waveguide, Marcuvitz (1951). The fields in the waveguide part of the antenna (inside the metamaterial tube) are represented in terms of the longitudinal components of the Hertz vector (see table),

For even TE modes	For odd TE modes
$\Pi_z = A_1 \sin(k_1 x) e^{ihz}$, for $\lvert x\rvert < a_1$ (20);	$\Pi_z = A_1 \cos(k_1 x) e^{ihz}$, for $\lvert x\rvert < a_1$ (23);
$\Pi_z = (B\sin(k_2 x) + C\cos(k_2 x)) e^{ihz}$, for $a_1 < \lvert x\rvert < a_2$ (21);	$\Pi_z = (B\sin(k_2 x) + C\cos(k_2 x)) e^{ihz}$, for $a_1 < \lvert x\rvert < a_2$ (24);
$\Pi_z = De^{-k_3\lvert x\rvert} e^{ihz}$, for $\lvert x\rvert > a_2$ (22);	$\Pi_z = De^{-k_3\lvert x\rvert} e^{ihz}$, for $\lvert x\rvert > a_2$ (25),

Table 1.

where
$$k_1 = \sqrt{k_0^2 \varepsilon_0 \mu_0 - h^2} \quad (26)$$

$$k_2 = \sqrt{k_0^2 \varepsilon \mu - h^2} \quad (27)$$

$$k_3 = \sqrt{h^2 - k_0^2 \varepsilon_0 \mu_0} \quad (28)$$

h is the longitudinal wavenumber; k_0 is the wavenumber in a vacuum; ε_0 and μ_0 are the permittivity and permeability of free space, respectively; ε and μ are the relative permittivity and permeability of the metamaterial, respectively; and *A*, *B*, *C*, and *D* are constants.

Hereinafter, the time dependent factor $e^{-i\omega t}$ is omitted.

The continuity boundary conditions for the tangential components at the $x = a_1$ and $x = a_2$ interfaces allow us to obtain the characteristic equations for the waveguide modes. It is also necessary to use the continuity condition for the longitudinal wavenumber *h*. The

characteristic equation allows us to find the longitudinal wavenumber h and the types of the modes propagating in the metamaterial waveguide. Figure 22 presents the values of h as a function of the tube thickness d for main modes of waveguide.

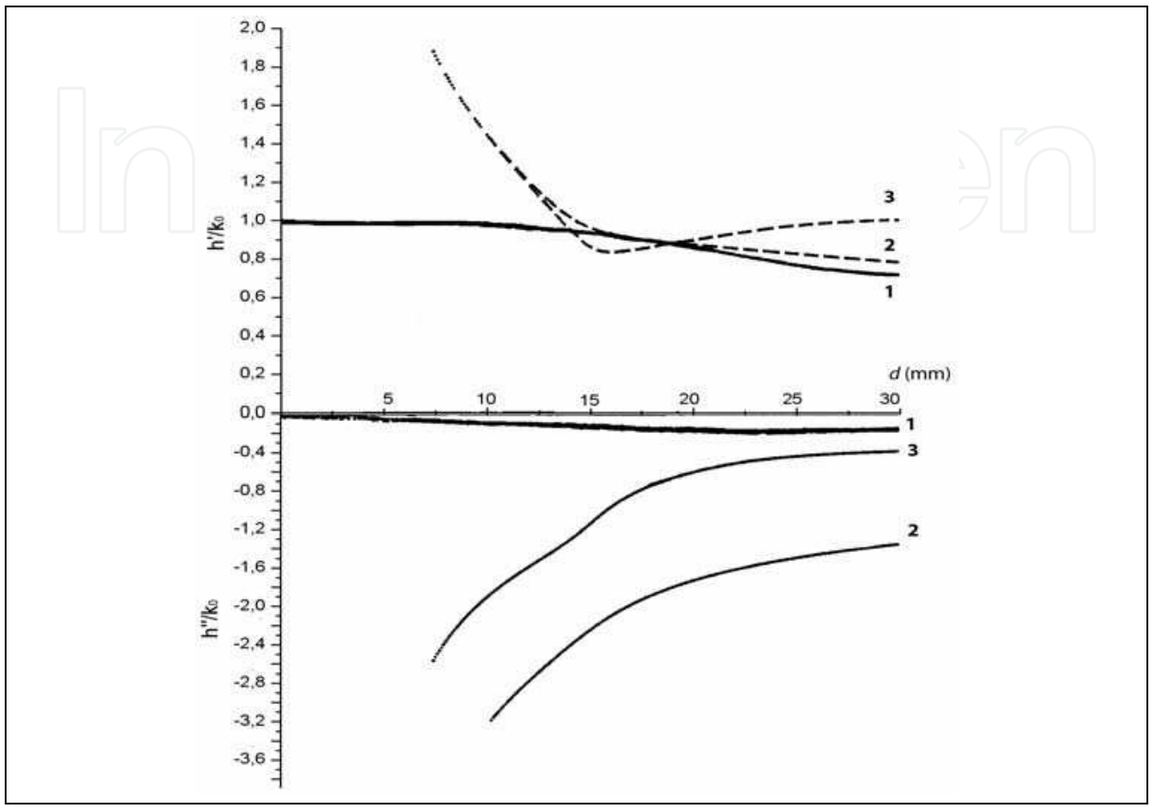

Fig. 22. Solution of the characteristic equation.

Here h` - the relative part, h`` an imaginary part of cross-section wave number h, normalized on k_0. In the waveguide supports forward, backward, and standing waves. The forward wave 1 corresponds to a wave extending in free space, waves 2 and 3- backward. In the beginning, the wave 1- dominates, and a total flux positive. Since some thickness thickness d, a wave 2 and 3 prevail also a total flux becomes negative.

The power flux in the central part of the waveguide and the surrounding waveguide free space is positive. Because of the negative values of permittivity and permeability, the flux is negative in the layer of metamaterial. Thus total power flux (in the cross section of the waveguide and the surrounding waveguide space) can be positive, negative or zero, depending on the predominance of flux in a given layer, Alu and Engheta (2005).

In other words, if the total flux is positive, then the waveguide is excited by forward wave, if negative - the backward wave, and in the case of zero flux, a standing wave.

Let us consider the behavior of the total power flux, depending on the thickness of the tube d.

As a result the total power flux in such structure passes from positive in negative (Fig. 23).

The normalized plot of the total power flux S_Σ as a function of the tube thickness d at a frequency of 3 GHz (the region of negative permittivity and permeability) is shown in Fig. 23. Clearly, the total power flux S_Σ may be positive (d < 10 mm), negative (d > 10 mm), or zero ($d \approx 10$ mm).

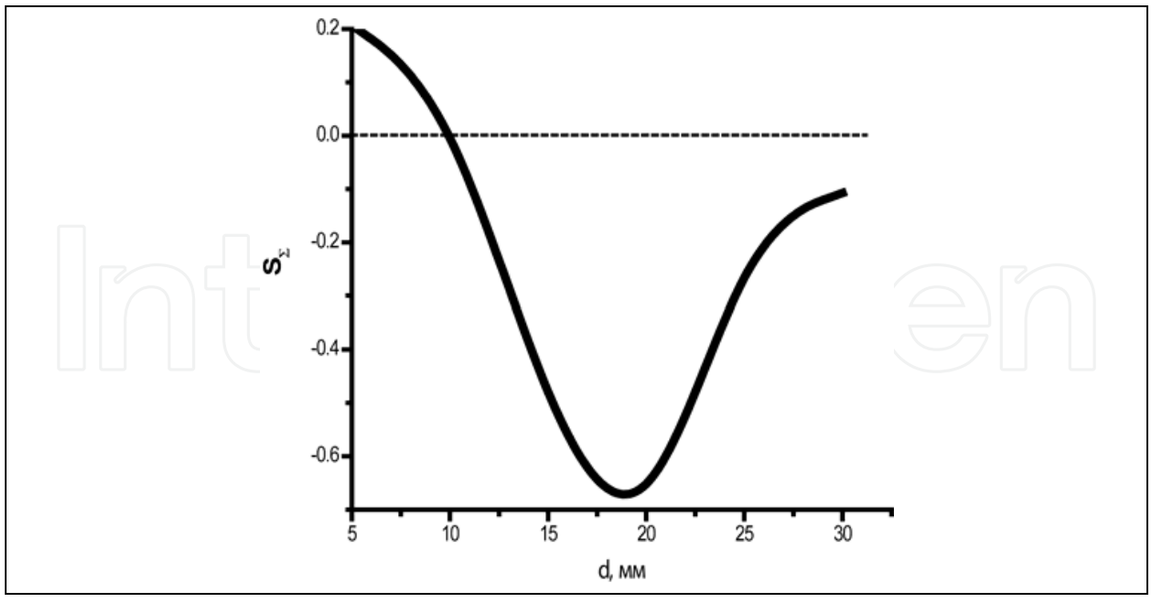

Fig. 23. Total power flux S_Σ versus the tube thickness d.

We have previously shown that when radiation is a single-layered planar metamaterial waveguide in the case of maintenance of the forward wave, the Radiation pattern has a maximum in the main direction. In the case of backward-wave waveguide radiates in the opposite direction, Basharin et al., 2010. Also proved, that the radiation in the opposite direction is possible only in the region of negative permittivity and permeability. It can be assumed that the existence of backward wave, two-layer waveguide radiates in the opposite direction.

6. The radiation from a metamaterial waveguide structure

Figures 24–28 present the normalized (to the maximum value in dB) radiation patterns (the field amplitudes as functions of the angular variable θ indicated in Fig. 18) of the rectangular metamaterial tube waveguide antenna excited through the coaxial waveguide adapter that were obtained by (dashed lines) numerical simulation with the use of the Method of Moments by Balanis (1997) and (solid lines) the measurements of the radiation pattern of the antenna in an anechoic chamber at frequencies close to the 3 GHz resonance frequency of the metamaterial. The difference between the measured and calculated diagrams may be as high as 5 dB.

Let us analyze the form of the radiation pattern of this waveguide antenna with various tube thicknesses d. At the tube thickness d < 10 mm, the total power flux is positive (see Fig. 24). According to Wu et al. (2003), Shevchenko (2005), a forward wave propagates in the waveguide in the 0° direction. Figure 24 shows the radiation pattern of the metamaterial tube antenna with the thickness d =5 mm at a frequency of 3 GHz.

The value d = 10 mm corresponds to zero total power flux S_Σ. A standing wave is formed in the waveguide, which results from the interference of the forward and backward waves whose longitudinal wave numbers h are equal in magnitude and opposite in sign. This corresponds to the radiation pattern of the waveguide antenna in which the front lobe is approximately equal to the back lobe (Fig. 25).

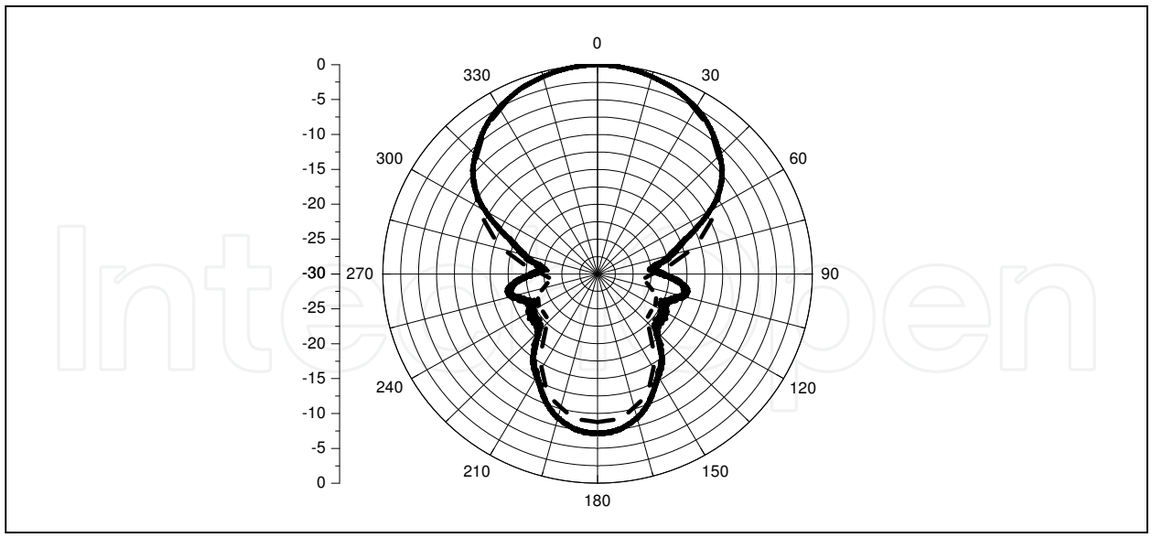

Fig. 24. Radiation pattern of the metamaterial tube waveguide antenna with the thickness d = 5 mm at a frequency of 3 GHz.

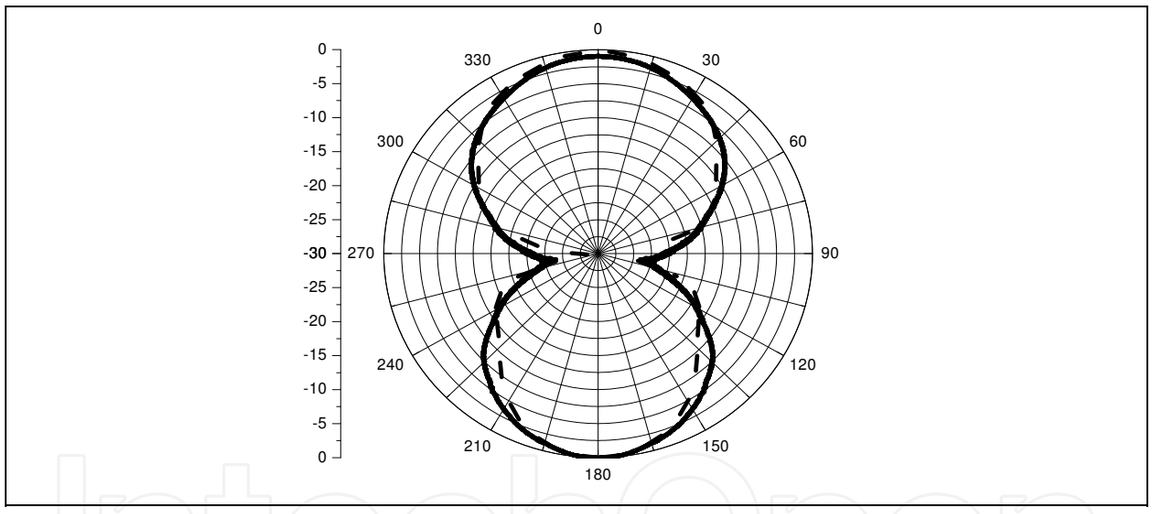

Fig. 25. Radiation pattern of the metamaterial tube waveguide antenna with the thickness d = 10 mm at a frequency of 3 GHz.

The thickness d > 10 mm of the metamaterial waveguide tube corresponds to the negative total power flux S_Σ; i.e., the wave propagates in the backward direction (180°). This corresponds to an increase in the amplitude of the back lobe and the "degeneration" of the main lobe. Figures 26, 27 are plotted for d = 15, 20 mm, respectively. At a thickness of 20 mm (Fig. 27), the difference between the back and front lobes of the radiation pattern is more than 15 dB and the antenna radiates predominantly in the backward direction 180°.

Thus, in the case of zero total power flux in the metamaterial waveguide, the antenna radiates equally in the directions 0° and 180°. In the presence of the forward and backward wave fields, the antenna radiates in the forward (0°) and backward (180°) directions, respectively.

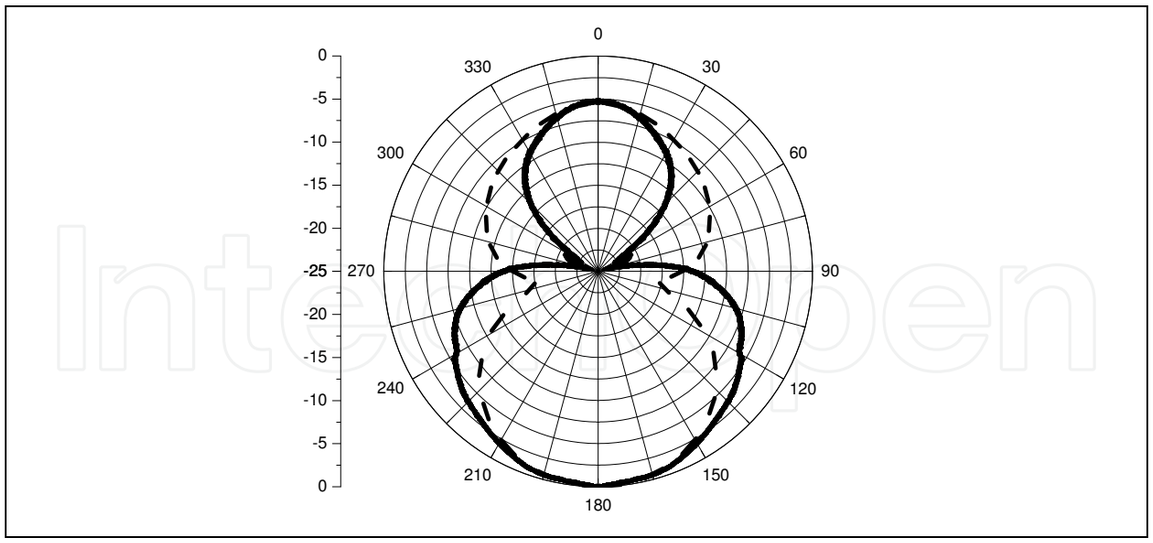

Fig. 26. Radiation pattern of the metamaterial tube waveguide antenna with the thickness d = 15 mm at a frequency of 3 GHz.

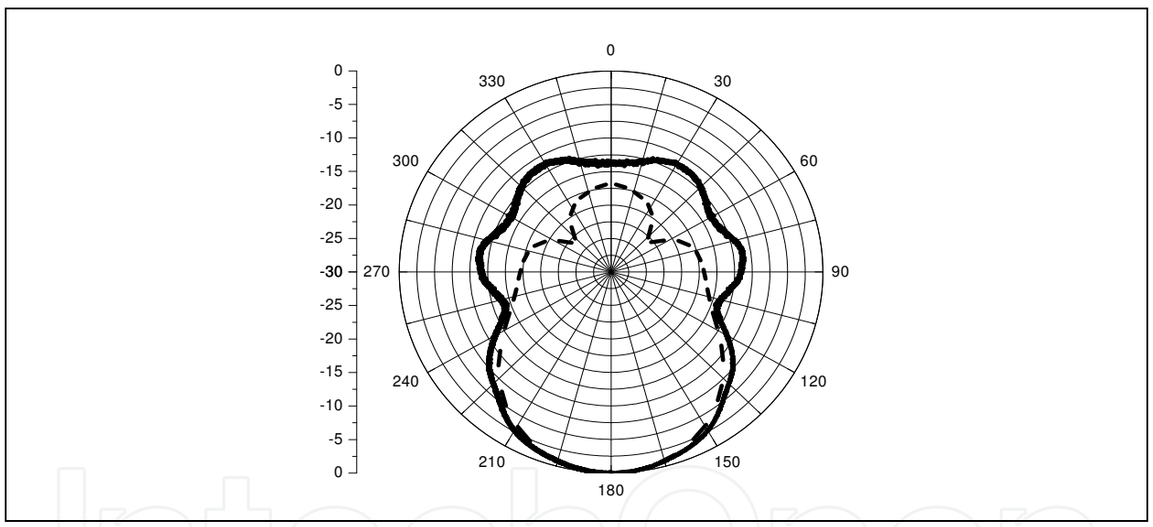

Fig. 27. Radiation pattern of the metamaterial tube waveguide antenna with the thickness d = 20 mm at a frequency of 3 GHz.

The backward radiation effect is observed only at the negative values of the real parts of permittivity and permeability. Figure 28 presents the radiation pattern of the metamaterial waveguide tube with the thickness d = 20 mm at a frequency of 3.5 GHz, for which permittivity and permeability are positive according to Fig. 21.

In this case, the radiation pattern is usual with the main lobe greater than the back lobe. That is, the antenna radiates mainly in the forward direction. To conclude, we have experimentally demonstrated the effect of the backward electromagnetic radiation of the metamaterial waveguide tube antenna. We have shown that the effect is observed in the presence of a backward wave field for the negative permittivity and permeability of the metamaterial, whereas the effect does not occur for the positive material parameters.

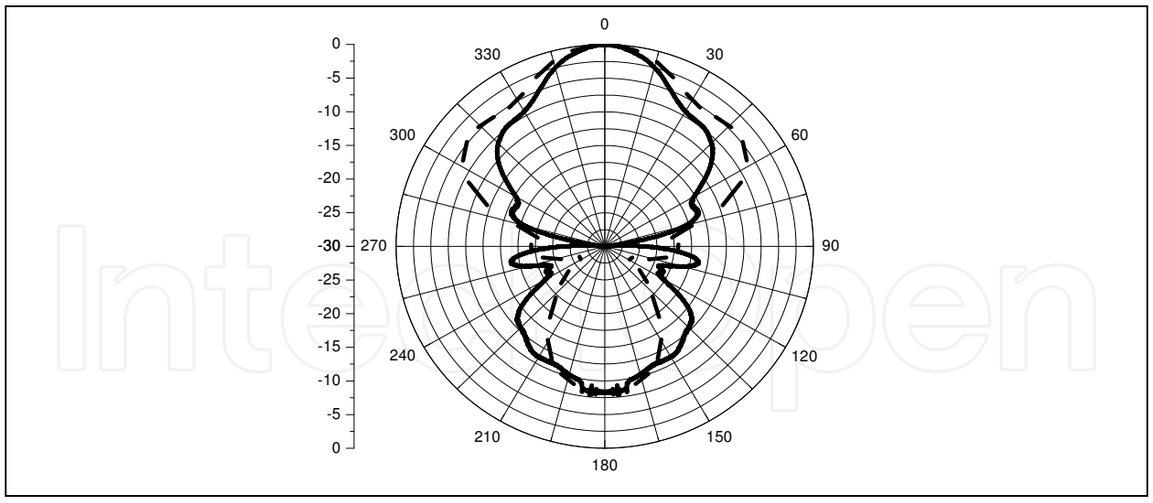

Fig. 28. Radiation pattern of the metamaterial tube waveguide antenna with the thickness d = 20 mm at a frequency of 3.5 GHz.

Next, we show that only the backward wave is the cause of the backward radiation effect. Of course, the radiation of the waveguide also contributes to the reflection from the open end. But the dimensions of the metamaterial waveguide are chosen so that the influence of reflected waves can be neglected, Volakis (2007), Angulo (1957).

We make a numerical experiment (MoM). Take our waveguide structure of the metamaterial (Fig. 18, 19), with the thickness of the tube $d = 20\ mm$, and construct the E field distribution on frequency 3 GHz (ε=-1.5+i0.7, μ=-0.7+i0.4) in the three cases. 1) the open end of the waveguide (Fig. 29 a), 2) the open end of the waveguide with a reflection coefficient of zero (Perfectly matched layers) (Fig. 29 b), 3) open end of the waveguide with a reflection coefficient of one (Perfectly conducting surfaces) (Fig. 29 c). A comparison of figures (Fig. 29) shows that the structure radiates the same in the direction 180^0 for all cases. In the case 1 (Fig. 29 a) part of the wave of the leak in the direction 0^0. In case 2 (Fig. 29 b), the wave is not

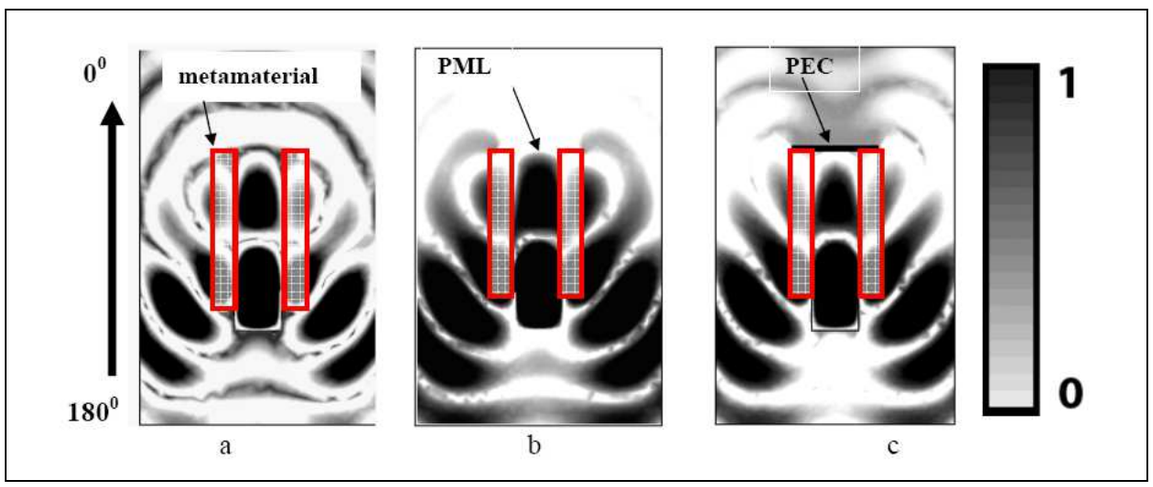

Fig. 29. Normalize electric field E. a) the open end of the waveguide, b) the open end of the waveguide with a reflection coefficient of zero (Perfectly matched layers), c) open end of the waveguide with a reflection coefficient of one (Perfectly conducting surfaces).

reflected from the end of the waveguide, and are absorbed in the PML and the radiation in the direction 0^0 of can be neglected. In case 3 (Fig. 29 c), there is diffraction on a conducting surface, which forms a small part of radiation in the direction 0^0 and in the direction 180^0.
Thus, the reflection from the open end of the metamaterial waveguide introduces a small perturbation in the total field, which does not affect the formation of reverse radiation. As a result, the main cause of back radiation is excited in the waveguide backward wave and the presence of negative permittivity and permeability.
Note that similar effect observed Sheng et al. (2009) by experimental modelling of the reversed Cherenkov radiations.
Propagation of electromagnetic waves in a metamaterial waveguide with negative values of the relative permittivity and relative permeability has been studied. It has been shown, that this waveguide can support forward, backward, and standing waves. In the case of the forward wave, an antenna manufactured on the basis of such a waveguide can radiate in a direction of 0°. In the case of the backward wave, the backward radiation effect is observed, i.e., the radiation pattern is formed in a direction of 180°. The condition for the backward radiation effect in the antennas built on the basis of metamaterial waveguides has been obtained. As follows from this condition, the backward radiation effect arises only in the antennas manufactured on the basis of waveguides consisting of metamaterials with negative values of the relative permittivity and relative permeability in the case of propagation of the backward wave.

7. Conclusion

Propagation of electromagnetic waves in a planar metamaterial waveguide with negative values of the relative permittivity and relative permeability has been studied. It has been shown, that this waveguide can support forward, backward, and standing waves. In the case of the forward wave, an antenna manufactured on the basis of such a waveguide can radiate in a direction of 0°. In the case of the backward wave, the backward radiation effect is observed, i.e., the radiation pattern is formed in a direction of 180°. The condition for the backward radiation effect in the antennas built on the basis of metamaterial waveguides has been obtained. As follows from this condition, the backward radiation effect arises only in the antennas manufactured on the basis of waveguides consisting of metamaterials with negative values of the relative permittivity and relative permeability in the case of propagation of the backward wave. The possibility of the preferential backward radiation of the structure has been shown on the basis of numerical calculations with the use of the method of moments and the measurements of the radiation pattern of the antenna in an anechoic chamber at frequencies close to the 3 GHz resonance frequency of the metamaterial.

8. Acknowledgements

Authors express their thanks to Vinogradov A.P. and Shevchenko V.V. for useful discussion.

9. References

Aizenberg G. Z. (1977), *Antennas UHF*, Svyaz, Moscow.
Alù A. and N. Engheta (2007a), Anomalies of subdiffractive guided wave propagation along metamaterial nanocomponents, *Radio Sci.*, *42*, RS6S17, doi:10.1029/2007RS003691.

Alù A. and Engheta N. (2005), "An Overview of Salient Properties of Planar Guided-Wave Structures with Double-Negative (DNG) and Single-Negative (SNG) Layers," *Negative-Refraction Metamaterials: Fundamental Principles and Applications*, G. V. Eleftheriades and K. G. Balmain (Ed.),IEEE Press, John Wiley and Sons Inc., Hoboken, NJ, Chapter 9, 339-380.

Alù A., Bilotti F., Engheta N., Vegni L.(2007b), *IEEE Trans*.. V. AP-55. No 6, P. 1698.

Angulo C. M. (1957), *IRE Trans. Microwave Theory Tech.* 5, 1.

P. Baccarelli, P. Burghignoli, G. Lovat, and S. Paulotto (2003), *IEEE Antennas Wireless Propag. Letter.*, Vol. 2, no 19., pp. 269-272.

Balabukha N. P., Basharin A. A., and Semenenko V. N. (2009), *JETP Letters*, vol. 89, no. 10, pp. 500-505.

Balanis C. A. (1997), *Antenna Theory: Analysis and Design,*Wiley, New York.

Basharin A.A., Balabukha N.P., and Semenenko V.N. (2010), *J. Appl. Phys*. 107, 113301.

Caloz C., Itoh T., (2006), *Electromagnetic metamaterials: transmission line theory and microwave - applications*. N.Y.: John Wiley and Sons, Inc.

Grbic A. and Eleftheriades G. V. (2002), *J. Appl. Phys*. 92, 5930.

Gulyaev Yu. V., Lagar'kov A. N., and Nikitov S. A. (2008), *Vestn. RAN* , 78 (5).

Hanson, G., and A. Yakovlev (1999), Investigation of mode interaction on planar dielectric waveguides with loss and gain, Radio Sci., 34(6), 1349-1359.

Katin S.V., Titarenko A.A. (2006), *Antennas*. Vol 5. (108). p.24-27.

Lagarkov A. N. (1990), *Electrophysical Properties of Percolation Systems*, IVTAN, Moscow, [in Russian].

Lagarkov A.N., Semenenko V.N., Chistyaev V.A. et al (1997), *Electromagnetics*. V.17. P 213

Lagarkov A.N., Semenenko V. N., Kisel V. N., and Chistyaev V. A. (2003), *J. Magn. Magn Mater*. V 161, P 258–259.

Lagarkov A.N., Kissel V.N (2004), *Phys. Rev. Lett.* V.92. P.077401.

Marcuvitz N. (1951), *Waveguide Handbook,* MCGraw-Hill, New York.

Muller D.E. (1965).Mathematical Tables and Aids to Computation. T.10. P.208.

Nefedov, I. S. and S. A. Tretyakov (2003), Waveguide containing a backward wave slab, *Radio Sci.*, *38*, 1101, doi:10.1029/2003RS002900I.

Pendry J.B. (2000), *Phys. Rev. Lett*.. V.85. P.3966

Shadrivov W., Sukhorukov A.A., and Kivshar Y.S. (2003), *Phys. Rev. E*, vol 67, pp.57602-1-57602-4

Shatrov A.D., Shevchenko V.V (1974), Radiophysics.. Vol. 11. C.1692.

Sheng Xi, Hongsheng Chen, Tao Jiang, Lixin Ran, Jiangtao Huangfu, Bae-Ian Wu, Jin Au Kong, and Min Chen (2009), Phys. Rev. Lett. 103, 194801.

Shevchenko V.V. (1969), *Radiotekh. Elektron*., Vol.50, P.1768

Shevchenko V.V (2005), *Radiotekh. Elektron*... Vol. 50. p. 1363.

Shevchenko V.V. Radiotekh. Elektron. (2000), Vol. 10. p. 1157

Smith D.R., Padilla W.T., Vier D.C. et al. (2000), *Phys. Rev. Lett*. V. 84. P. 584.

Solymar L., Shamonina E. (2009), Waves in Metamaterials, OXFORD Press, New York.

Vainshtein L. A. (1988), *Electromagnetic Waves* (Radio I Svyaz', Moscow,) [in Russian].

Veselago V. G. (1967), *Usp. Fiz. Nauk*, Vol. 92, P. 517

Volakis J. A. (2007), *Antenna Engineering Handbook*, 4th ed., McGraw-Hill, New York,.

Wu B.-I., Grzegorczyk T. M., Zhang Y., and Kong J. A., *J. Appl. Phys* (2003), Vol. 93, P. 9386.

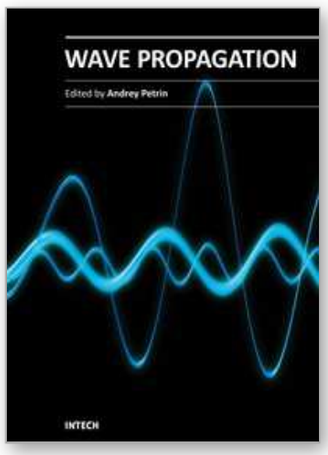

Wave Propagation
Edited by Dr. Andrey Petrin

ISBN 978-953-307-275-3
Hard cover, 570 pages
Publisher InTech
Published online 16, March, 2011
Published in print edition March, 2011

The book collects original and innovative research studies of the experienced and actively working scientists in the field of wave propagation which produced new methods in this area of research and obtained new and important results. Every chapter of this book is the result of the authors achieved in the particular field of research. The themes of the studies vary from investigation on modern applications such as metamaterials, photonic crystals and nanofocusing of light to the traditional engineering applications of electrodynamics such as antennas, waveguides and radar investigations.

How to reference
In order to correctly reference this scholarly work, feel free to copy and paste the following:

Alexey A. Basharin, Nikolay P. Balabukha, Vladimir N. Semenenko and Nikolay L. Menshikh (2011). Metamaterial Waveguides and Antennas, Wave Propagation, Dr. Andrey Petrin (Ed.), ISBN: 978-953-307-275-3, InTech, Available from: http://www.intechopen.com/books/wave-propagation/metamaterial-waveguides-and-antennas

INTECH
open science | open minds

InTech Europe
University Campus STeP Ri
Slavka Krautzeka 83/A
51000 Rijeka, Croatia
Phone: +385 (51) 770 447
Fax: +385 (51) 686 166
www.intechopen.com

InTech China
Unit 405, Office Block, Hotel Equatorial Shanghai
No.65, Yan An Road (West), Shanghai, 200040, China
中国上海市延安西路65号上海国际贵都大饭店办公楼405单元
Phone: +86-21-62489820
Fax: +86-21-62489821

IntechOpen